Carbohydrate Polymers 89 (2012) 423–431

Contents lists available at SciVerse ScienceDirect

Carbohydrate Polymers

journal homepage: www.elsevier.com/locate/carbpol

Effect of lignin content on a GH11 endoxylanase acting on glucuronoarabinoxylan-lignin nanocomposites

Imen Boukari [a,b], Caroline Rémond [a,b], Michael O'Donohue [c,d,e], Brigitte Chabbert [a,b,*]

[a] INRA, UMR614 Fractionnement des AgroRessources et Environnement, F-51100 Reims, France
[b] Université de Reims Champagne-Ardenne, UMR614 Fractionnement des AgroRessources et Environnement, F-51100 Reims, France
[c] Université de Toulouse, INSA, UPS, INP, LISBP, F-31077 Toulouse, France
[d] INRA, UMR792 Ingénierie des Systèmes Biologiques et des Procédés, F-31400 France
[e] CNRS, UMR5504, F-31400 Toulouse, France

ARTICLE INFO

Article history:
Received 21 November 2011
Received in revised form 7 February 2012
Accepted 8 March 2012
Available online 19 March 2012

Keywords:
Lignin model compounds (DHP)
GH11 endoxylanase
Lignin–carbohydrate nanocomposites
Particle size
Enzyme inhibition
Adsorption surface

ABSTRACT

The effects of lignin content on the activity and action pattern of GH11 endoxylanase from *Thermobacillus xylanilyticus* were investigated using *in vitro* reconstituted non-covalent glucuronoarabinoxylan-model lignin (GAX-DHP) nanocomposites. Four types of nanocomposites were prepared, each displaying different lignin contents. Variations in the DHP (model lignin) polymerization process were induced by increasing the coniferyl alcohol concentration. Examination of the morphology of the nanocomposites revealed globular particles enrobed in a matrix. The size of these particles increased in line with the lignin concentration. Physicochemical characterization of the *in vitro* reconstituted GAX-DHPs strongly suggested that increased particle size is directly related to the solubility and reactivity of coniferyl alcohol, as reflected by changes in the amount of β-*O*-4 linkages. Evaluation of the impact of the GH11 endoxylanase on the GAX-DHP nanocomposites revealed a negative correlation between the proportion and organization patterns of DHP in the nanocomposites and enzyme activity.

1. Introduction

At present, lignocellulosic biomass is being promoted as a renewable feedstock for the production of fuels and value-added chemicals (McKendry, 2002). The bioconversion of biomass into fuels and chemicals involves several operations, including pretreatment and enzymatic hydrolysis, which aim to deconstruct the biomass, mainly into fermentable sugars. Nevertheless, the enzymatic digestibility of lignocelluloses is largely affected by several limiting factors. Although the determinants of these limitations have not been elucidated unambiguously, these factors have traditionally been divided into two groups: biomass structural features and enzyme mechanisms (Anderson & Akin, 2008; Zhu, O'Dwyer, Chang, Granda, & Holtzapple, 2008).

Regarding biomass structure, it has been established that enzyme accessibility and efficiency are affected by a number of factors, including cellulose crystallinity, the degree of polymerization and substitution of hemicelluloses and lignin content and distribution (Chang & Holtzapple, 2000; Wyman, 2003). However, it is generally considered that lignin is the most important obstacle to be overcome by biomass-degrading enzymes. Research has shown that biomass digestibility is negatively correlated with the lignin content and can be enhanced by increasing lignin removal through pre-treatments (Chandra et al., 2007; Chang & Holtzapple, 2000; Draude, Kurniawan, & Duff, 2001). To date, the principal advances in our understanding of the effects of lignin on the action of cellulases and hemicellulases have been based on the use of particulate, isolated lignin samples derived from various botanical sources using different extraction methods (organosolv softwood lignins, alkali-extracted lignins, *etc.*) and/or soluble lignin degradation products produced during industrial applications (pulping liquors, *etc.*) (Berlin et al., 2006; Kaya, Heitmann, & Joyce, 1999; Senior, Mayers, Breuil, & Saddler, 1990). However, owing to the low solubility of lignins in aqueous systems, the use of organic solvents is usually necessary, which might affect enzyme stability and/or activity. Moreover, the heterogeneous nature and variability of lignocellulosic biomass, and the multiplicity of the enzymes needed to degrade it, render the study of enzyme inhibition quite difficult, because it is complicated to assess the relative contribution of multiple limiting factors. Therefore, the use of simplified, biomimetic model systems is an attractive alternative to study the influence of lignins on enzyme activity.

Abbreviations: CA, coniferyl alcohol; GAX, glucuronoarabinoxylan; DHPs, dehydrogenation polymers; SEC, size exclusion chromatography; M_w, average molecular weight; THF, tetrahydrofuran.

* Corresponding author at: UMR614, INRA, 2 esplanade Roland Garros, 51100 Reims Cedex, France. Tel.: +33 3 26 77 35 94; fax: +33 3 26 77 35 99.
E-mail address: chabbert@reims.inra.fr (B. Chabbert).

0144-8617/$ – see front matter © 2012 Elsevier Ltd. All rights reserved.
doi:10.1016/j.carbpol.2012.03.024

Lignin is formed through an enzyme-initiated but chemically controlled dehydrogenation reaction (Sarkanen, 1971). This dehydrogenation process can be reproduced *in vitro* by the synthesis of Dehydrogenation Polymers (DHPs) generated by the oxidative polymerization of monolignols using either peroxidase or laccase (Freudenberg & Neish, 1968). This *in vitro* reaction has been used advantageously to study the effects of different physicochemical parameters on the final lignin polymer. For instance, the influence of how the reactants are added (bulk (Zulaufverfahren; ZL) or end-wise (Zutropfverfahren; ZT) mode), the type of monomer used, the oxidizing enzyme, the prevailing pH and the presence (at variable concentrations) of polysaccharides are among the reaction variables that have been investigated. Through these studies, it is known that the synthesis of DHP in the presence of polysaccharides leads to the formation of a colloidal complex which prevents lignin precipitation (Barakat, Chabbert, & Cathala, 2007; Cathala & Monties, 2001; Higuchi, Ogino, & Tanahashi, 1971).

In a previous work (Boukari et al., 2009), glucuronoarabinoxylan-lignin (GAX-DHP) nanocomposites were prepared *in vitro* and studied with regard to the action patterns of a GH11 endoxylanase. To further pursue this goal, we describe here the action of a GH11 endoxylanase on nanocomposites of GAX-DHP that display variable lignin contents (DHP). These nanocomposite systems thus allowed us to study the impact of lignins interacting with hemicelluloses rather than with single polymer. Moreover, to better appreciate the sole impact of lignins on enzyme hydrolysis, the GAX-DHP complexes thus synthesized were almost free of intermolecular covalent linkages.

2. Materials and methods

2.1. Materials

Delignified water soluble glucuronoarabinoxylans (GAX) were obtained from oat spelt as previously described (Winter, Barakat, Cathala, & Saake, 2006); briefly, after extraction with 5% (w/v) NaOH at 90 °C, further purification by washing with methanol/water (60/40, v/v), methanol and ether and finally ClO_2 bleaching at 70 °C and recovery of the water-soluble polymer fraction. Basically, the GAX sample displayed an average molecular weight of 22.650 g/mol, an arabinose/xylose ratio of 0.23, a 4-methyl glucuronic acid content of 8.2% and a lignin content estimated at 4.9% (Winter et al., 2006).

The thermostable GH11 endoxylanase (Tx-Xyl) was produced from *Thermobacillus xylanilyticus* (previously designed *Bacillus* sp. D3) (Samain, Debeire, & Touzel, 1997; Samain, Touzel, Brodel, & Debeire, 1992) and purified to homogeneity using a two-step chromatographic procedure (ion-exchange (Q Sepharose fast flow) followed by hydrophobic interaction (phenyl Sepharose CL4B) chromatography) according to the previously established protocol (Debeire-Gosselin, Loonis, Samain, & Debeire, 1992). The specific activity of the pure protein was about 2000 IU/mg protein, where one IU is defined as the amount of endoxylanase required to release 1 μmol of reducing xylose equivalent from birchwood xylan per min at 60 °C.

2.2. Synthesis of GAX-lignin (DHP) model complexes

Dehydrogenation polymers (DHP) are synthetic analogs of lignins. They are obtained *in vitro* by the oxidative polymerization of lignin monomers. During this study, we synthesized DHP by polymerizing coniferyl alcohol using horseradish peroxidase (HRP type VI, E 1.11.1.7, 250–300 unit/mg, purchased from Sigma. One unit forms 1.0 mg purpurogallin from pyrogallol in 20 s at pH 6.0 and 20 °C) and hydrogen peroxide in the presence of glucuronoarabinoxylan (GAX) (4 g/L), according to the Zulaufverfahren method (Tanahashi & Higuchi, 1982).

The coniferyl alcohol (CA) (4-hydroxy-3-methoxy cinnamyl alcohol) used for this synthesis was prepared according to the procedure described by Ludley and Ralph (Ludley & Ralph, 1996).

Four polymerization experiments were performed, with increasing CA concentrations. Thus, three solutions were prepared as follows:

- Solution 1: Solution of GAX (4 g/L) in water (pH 5.0).
- Solution(s) 2: 12.5, 50, 200 and 400 mg of CA dissolved separately in 3 mL dioxane and 9.5 mL of Solution 1.
- Solution 3: 12.5 mL of Solution 1 containing hydrogen peroxide (H_2O_2) (2 equiv. compared to coniferyl alcohol, 13.5, 50, 200 and 400 μL, respectively).

Before polymerization, appropriate amounts of horseradish peroxidase were added to (4×) 25 mL of Solution 1 (0.5, 2.5, 10 and 20 mg, respectively), thus maintaining the peroxidase/CA *ratio* constant. The reactions were started by adding solutions 2 and 3 simultaneously to solution 1 (50 mL final volume) according to the bulk (Zulaufverfahren or ZL) polymerization method, and the mixtures were left to react under continuous stirring for 16 h at 25 °C. The synthesis yielded four stable colloidal suspensions of GAX-DHP model complexes: GAX-DHP (4/0.25, w/w), GAX-DHP (4/1, w/w), GAX-DHP (4/4, w/w) and GAX-DHP (4/8, w/w), corresponding to CA concentrations of 0.25, 1, 4 and 8 g/L, respectively.

2.3. Extraction of DHP molecules from GAX-DHP complexes

After freeze drying, GAX-DHP complexes were dissolved in dioxane–water (95:5) and soluble DHP molecules were recovered a fter centrifugation (at 13,000 rpm, 10 min). Yields of the extractions, determined spectrophotometrically with respect to the total initial CA, were 62.7%, 68.3%, 85.4% and 95.4%, respectively for GAX-DHP (4/0.25), GAX-DHP (4/1), GAX-DHP (4/4) and GAX-DHP (4/8). The DHP fractions were then washed three times with distilled water and freeze dried prior to subsequent analysis by thioacidolysis and size exclusion chromatography (SEC).

2.4. Size-exclusion chromatography (SEC) analysis of DHP samples in THF

Prior to SEC analysis, the dioxane–water extracted DHP fractions were acetylated with a mixture of acetic anhydride and pyridine (1/1, v/v) for 24 h at 40 °C. The reaction products were then poured into iced water and extracted with dichloromethane. Organic layers were washed with dilute hydrochloric acid, saturated sodium bicarbonate solutions and finally water. The organic fractions were dried over magnesium sulfate and concentrated under reduced pressure to give the acetylated DHP samples.

SEC analyses were performed using a multi-detection system consisting of a pump (model 510, Waters), an auto-sampler (U6K injector, Waters), two Polymer Laboratories columns (PLgel Mixed D, 5 μ 300 mm × 7.5 mm) and a UV-detector (Waters 2996). Separation was performed in tetrahydrofuran (THF) by injecting 100–200 μl of acetylated samples (1 g/L) into the thermostatically controlled PLgel columns (40 °C) at a flow rate of 1 mL/min. Detection was carried out at 280 nm. Molar mass evaluation (M_w and M_n) was based on the relative calibration method using polystyrene standards (Shodex Standard SL-105).

2.5. Thioacidolysis

Dioxane–water extracted DHP fractions were degraded by thioacidolysis to estimate the content of β-*O*-4 linked structures according to Lapierre's procedure (Lapierre, Monties, & Rolando, 1986).

This procedure consists in acid-catalysed solvolysis in dioxan/ethanethiol with boron trifluoride, which results in the cleavage of aryl-glycerol β-aryl ether (*β-O*-4) linkages.

The main degradation products (tri-thioethyl phenylpropane compounds) of the different DHP fractions, as well as the proportion of coniferyl alcohol end-groups units linked at C_4OH, were quantified as trimethylsilyl (TMS) derivatives by gas chromatography using flame-ionization detection (FID) with a J&W Scientific column (DB 1, 30 m, 0.25 mm, 0.25 μm film) and tetracosane as the internal standard. Lignin monomer derivatives were identified by gas chromatography separation and mass spectrometry (Polaris Q Thermo) according to the technique described by Lapierre (1993).

2.6. Transmission electron microscopy (TEM)

Droplets of GAX-DHP suspensions were deposited on glow-discharged carbon-coated grids. Any excess liquid was blotted away with filter paper and a drop of 2% (w/v) uranyl acetate negative stain was added prior to drying. The samples were observed using a Philips CM200 microscope operating at 80 kV. Images were recorded and particle diameters were measured using ImageJ software.

2.7. Endoxylanase (Tx-Xyl) assays

The kinetics of enzymatic hydrolysis of the free delignified GAX and GAX-DHP model complexes were determined under continuous stirring at 60 °C for 10 min in a final volume of 15 mL. Limiting amounts of Tx-Xyl (0.04 IU/mg GAX) were used in order to compare the relative activity and monitor the enzyme activity pattern on each substrate. For all tests, the substrates were pre-incubated at 60 °C for 10 min before Tx-Xyl was added. After this, aliquots were removed from the reaction mixture at regular 2 min intervals, boiled for 10 min to inactivate Tx-Xyl and subjected to both SEC and reducing sugar analyses.

The relative activity (IU/mL) of Tx-Xyl toward GAX and GAX-DHP complexes was determined by measuring the amount of reducing sugars (xylose and xylo-oligosaccharides) released by the endoxylanase throughout the 10 min reaction. Reducing sugars were quantified as alditol acetates using gas-liquid chromatography according to the procedure developed by Courtin, Van den Broeck, and Delcour (2000)), but instead of trifluoroacetic acid, the samples were hydrolysed using sulfuric acid (1 M final concentration) at 100 °C for 2 h. Dichoromethane was used to extract the alditol acetates. Chromatographic analysis was performed using a gas chromatograph (GC Hewlett Packard 6890A) equipped with an auto-sampler and a flame ionizing detector. The separation of alditol acetates was achieved at 220 °C on a Supelco Sp-2380 polar column (0.25 mm × 30 m) using He (at 1 bar) as the carrier gas. Detection and injection were performed at 250 °C. Appropriate mixtures of monomeric reducing sugars were used for calibration and inositol was included as the internal standard.

Relative activity was expressed as IU/mL, where one IU is defined as the amount of endoxylanase required to release 1 μmol of reducing xylose equivalent from the substrate per min at 60 °C.

2.8. Size-exclusion chromatography (SEC) analysis of GAX-DHP complexes in $NaNO_3$

GAX and GAX-DHP complexes were analyzed before and after endoxylanase (Tx-Xyl) activity using a high performance size exclusion chromatographic (SEC) system, connected on-line to a UV detector (Waters 2996) and a refractive index detector (RI) (Waters 410). The chromatographic separation of 100 μl injected solutions (filtered on a 0.45 μm PTFE filter) was performed in an $NaNO_3$ solution (50 mM) containing 0.02% NaN_3, with thermostatically controlled (50 °C) Shodex OH pack columns (802, 803 and 805) (each 4.6 mm × 300 mm) set at a flow rate of 1 mL/min. Molar masses (M_w) were monitored during hydrolysis kinetics and evaluations were based on pullulan standards.

3. Results and discussion

3.1. Characterization of GAX-DHP complexes

In plant cell walls, lignin polymerization occurs within a polysaccharide matrix. Therefore, in order to mimic this process, DHPs were synthesized using coniferyl alcohol (CA) monomers in the presence of glucuronoarabinoxylan (GAX) (4 g/L). Four polymerization reactions were performed using identical GAX concentrations, pH values and peroxidase/H_2O_2 ratios, but employing increasing concentrations of lignin monomer (CA). Consistent with our previous findings (Barakat, Winter, et al., 2007; Boukari et al., 2009), no precipitation was observed during the polymerization reactions. The syntheses yielded four stable colloidal GAX-DHP model systems: GAX-DHP (4/0.25, w/w), GAX-DHP (4/1, w/w), GAX-DHP (4/4, w/w) and GAX-DHP (4/8, w/w), whose macromolecular properties were studied using size exclusion chromatography (SEC), TEM imaging and physicochemical characterization.

3.1.1. Size exclusion chromatography (SEC) analysis of GAX-DHP complexes

The macromolecular organization in solution of the different GAX-DHP nanocomposites was analyzed by SEC using an aqueous mobile phase ($NaNO_3$) and both RI and UV detection. Compared to GAX alone (Fig. 1a), the GAX-DHP complexes were characterized by polydisperse elution profiles, which varied according to the DHP monomer concentration in nanocomposites. Thus, in the case of GAX-DHP (4/0.25), a slight shoulder associated with the main peak (corresponding to the major GAX polymer eluted at 23 mL) appeared at 18 mL (Fig. 1b). Two additional peaks were also detected (at 17 and 19.5 mL elution volumes) for GAX-DHP (4/1) (Fig. 1c), and peaks of increasing intensity (eluted at 16 and 19 mL) were observed for GAX-DHP (4/4) and GAX-DHP (4/8), respectively (Fig. 1d and e). All of these peaks corresponded to high molecular weight populations that displayed both RI and UV signals. Given that DHPs were the only UV-absorbing components, but were at the same time insoluble in the aqueous eluent, it could be assumed that these fractions corresponded to micellar hydrosoluble populations formed by the association of hydrophilic, soluble GAX polymers and hydrophobic synthesized DHP molecules. These SEC patterns were consistent with previous results obtained from a similar synthesis of GAX-DHP using coniferyl alcohol (Boukari et al., 2009).

According to previous results (Barakat, Winter, et al., 2007), the GAX-DHP complexes described here would mainly involve non covalent hydrophobic interactions between the two components. During the synthesis process, these interactions drive the formation of soluble micelle-like structures that can maintain the originally insoluble DHP molecules in solution, as is the case of a surfactant system. The presence of GAX in solution will thus prevent the precipitation of lignin models during coniferyl alcohol polymerization (Barakat, Chabbert, et al., 2007; Cathala & Monties, 2001). This effect could be related to the "sugar in" effect observed by Shigematsu, Goto, Yoshida, Tanashi, and Shinoda (1994) who demonstrated that monolignol solubility is increased in sugar solutions.

Overall, our SEC analyses revealed that the different GAX-DHP nanocomposites contained a mixture of free GAX chains with non covalent GAX-DHP complexes. The increase in the intensities of both the RI and UV signals of the non-covalently associated

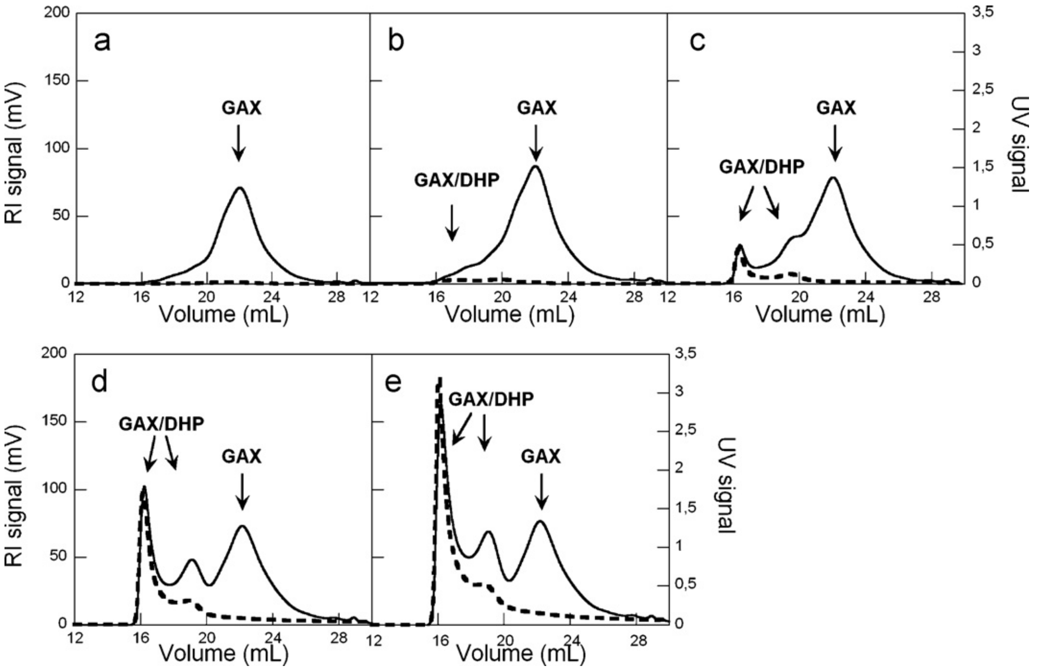

Fig. 1. SEC-NaNO$_3$ elution profiles of GAX-DHP model systems before Tx-Xyl treatment (a) GAX, (b) GAX-DHP (4/0.25), (c) GAX-DHP (4/1), (d) GAX-DHP (4/4), (e) GAX-DHP (4/8). (– – –): Refractive index (RI signal); (- - - - - -): Ultraviolet (UV signal).

GAX-DHP fractions (eluted at high molar mass volumes) indicated that these populations displayed increasing concentrations as the DHP levels increased within the nanocomposites when polymerizing rising concentrations of coniferyl alcohol (CA).

3.1.2. *Morphology and size distribution of GAX-DHP complexes*

Morphological characterization of the different GAX-DHP nanocomposites was achieved by TEM imaging. Typical images of negatively stained preparations indicated that the GAX-DHP nanocomposites appeared as individual spherical particles embedded in a matrix (Fig. 2). Such an organization is consistent with their amphiphilic nature, since they are formed by the non covalent assembly of somewhat hydrophilic GAX polymers (composed of poly-hydroxylated sugar subunits) and hydrophobic DHP compounds (composed of phenylpropane units with fewer hydroxyl groups). It is therefore reasonable to hypothesize that in an aqueous solution, they would be organized in a minimum energy surface, (*i.e.*, a sphere), as reported elsewhere (Micic, Radotic, Jeremic, Djikanovic, & Kämmer, 2004; Radotic, Micic, & Jeremic, 2005).

The size of the globular nanocomposites was determined by fitting the outline of each particle to an equivalent ellipse. The diameter was calculated as the average between the largest and smallest diameters of the ellipse. The number and weight average diameters ($\overline{D_n}$ and $\overline{D_w}$, respectively), as well as the polydispersity index P_d were calculated using the expressions presented previously by Putaux, Buléon, Borsali, and Chanzy (1999). Although the mean values measured may not exactly have been those of the systems in solution, since possible deformation after staining and drying could not totally be excluded, they provided a means to compare particle size. The size distribution histograms for GAX-DHP (4/1), GAX-DHP (4/4) and GAX-DHP (4/8) are shown in Fig. 3. These histograms are symmetrical and tend respectively toward increasingly larger diameters. Table 1 summarizes the diameter values obtained. The polydispersity indices revealed that several GAX-DHP particles were relatively homogeneous in diameter, and indicated that particle diameter increased in line with the DHP content. For instance, GAX-DHP (4/8) particles were almost twice as large as GAX-DHP (4/1) particles ($\overline{D_n} = 205.4$ nm and 113.5 nm, respectively). Interestingly, the SEC behavior of the different nanocomposites showed that the concentrations of GAX-DHP complexes (with high molar masses) rose as the DHP concentration increased. One might thus hypothesize that the particles corresponded to GAX-DHP micellar complexes. In this respect, the increased size of the particles perhaps reflected a higher frequency of non covalent interactions between GAX and growing DHP polymer (*i.e.* interfacial (hydrophilic/hydrophobic) and/or cooperative electrostatic interactions) (Barakat, Winter, et al., 2007; Micic, Radotic, Jeremic, & Leblanc, 2003), as well as a higher DHP content. Such a trend may have resulted from the combination of a higher concentration of DHP and an increased size of the DHP polymer within the composites.

3.1.3. *Characterization of DHP extracted from GAX-DHP complexes*

One of the consequences of coniferyl alcohol (CA) polymerization in the GAX solution should have been a greater solubility of the phenolic oligomers generated, which would otherwise have precipitated in the absence of a polysaccharide matrix (Barakat, Chabbert, et al., 2007; Cathala & Monties, 2001). In addition, increasing the monomer concentration within the polysaccharide matrix would allow more frequent coupling between oligomers, giving rise to final DHP polymers with higher molecular weights.

In order to check this hypothesis, DHP molecules were extracted from the respective GAX-DHP model systems by dioxane–water (95:5) and further subjected to molar mass determination (SEC) and chemical analysis (thioacidolysis). The extraction yields were 62.7%, 68.3%, 85.4% and 95.4%, respectively, for GAX-DHP (4/0.25),

Table 1
Mean number and weight diameters ($\overline{D_n}$ and $\overline{D_w}$, respectively), standard deviation (±) and polydispersity index (P_d) determined from TEM images of negatively stained GAX-DHP particles before Tx-Xyl treatment.

Sample	$\overline{D_n}$ (nm)	$\overline{D_w}$ (nm)	P_d
GAX-DHP (4/1)	113.5 ± 13.4	118.1	1.04
GAX-DHP (4/4)	159.9 ± 21.3	168.4	1.05
GAX-DHP (4/8)	205.4 ± 26.3	216.2	1.05

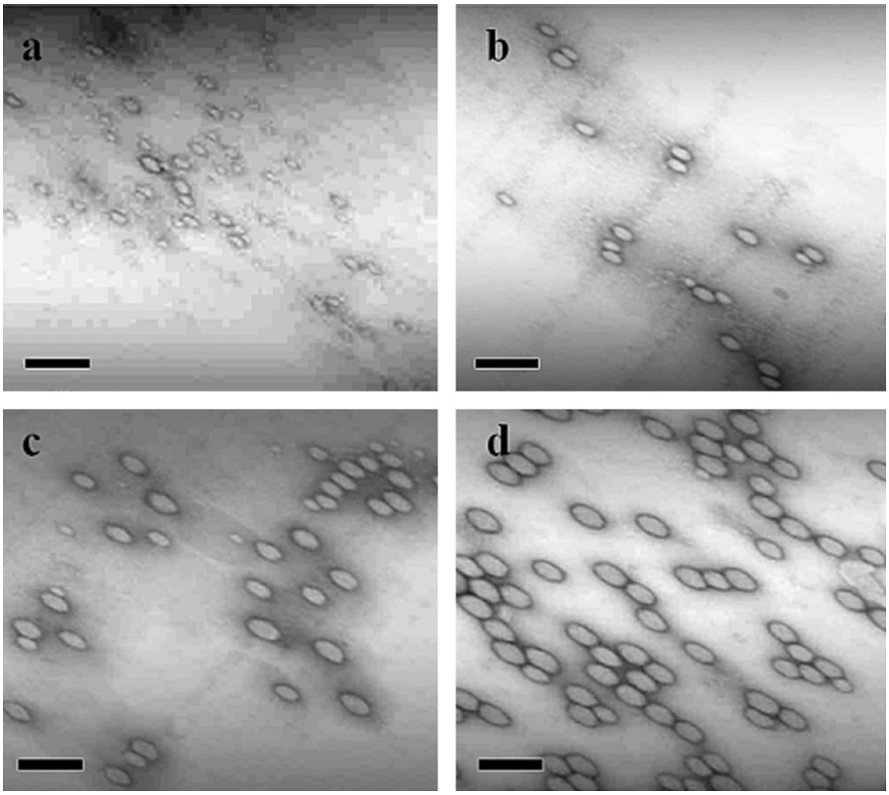

Fig. 2. TEM images of negatively stained GAX-DHP particles before Tx-Xyl treatment: (a) GAX-DHP (4/0.25), (b) GAX-DHP (4/1), (c) GAX-DHP (4/4) and (d) GAX-DHP (4/8). Scale bars: 500 nm.

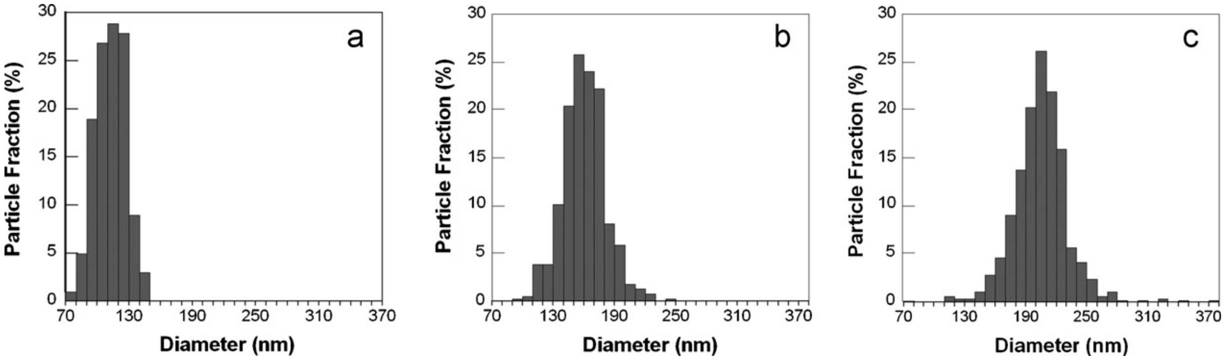

Fig. 3. Size-distribution histograms of GAX-DHP particles before Tx-Xyl treatment: (a) GAX-DHP (4/1), (b) GAX-DHP (4/4) and (c) GAX-DHP (4/8).

GAX-DHP (4/1), GAX-DHP (4/4) and GAX-DHP (4/8) (based on the initial CA concentration). These yields were relatively high, so such analyses would be significantly representative of the total DHPs formed. Furthermore, the extraction yields rose as the DHP/GAX *ratio* increased, because the residual carbohydrate content usually reduces DHP solubility in dioxane.

In order to evaluate the DHP molar mass, DHP fractions were acetylated and subjected to SEC analysis in THF. Using THF as an elution system decreases the interactions between DHP chains, thus preventing macromolecular associations and hence any overestimation of molecular weight (Chum, Johnson, Tucker, & Himmel, 1987; Faix & Lange, 1981). Higher molecular weight products were clearly detected in the case of DHP extracted from both GAX-DHP (4/8) and GAX-DHP (4/4) comparatively to GAX-DHP (4/1). The respective M_w values were calculated based on polystyrene calibration and are reported in Table 2. Consistent with the data available in the literature on DHP synthesized under similar conditions (Cathala, Saake, Faix, & Monties, 1998; Saake, Argyropoulos, Beinhoff, & Faix, 1996), the molecular weight of extracted DHPs ranged from 1800 to 2300 g/mol and rose in line with increasing DHP concentrations in the complexes, as previously reported with similar systems involving covalent linkages (Barakat, Chabbert,

Table 2
Characterization of the DHP extracted with dioxane–water (95:5) from the respective GAX/DHP (4/0.25; 4/1; 4/4; 4/8; *w*/*w*) complexes: Yield of thioethylated (*β*-*O*-4) monomers recovered from thioacidolysis and weight average molecular weight (M_w) determined from SEC-THF analysis.

Samples	*β*-*O*-4 (μmol/g of DHP)	M_w (g/mol)	*P*
DHP 0.25	154 ± 5	–	–
DHP 1	452 ± 14	1855	1.6
DHP 4	529 ± 7	2201	1.3
DHP 8	620 ± 1	2306	1.4

Thioacidolysis yields are mean values of duplicates (± standard error).
$P = M_w/M_n$: Polydispersity; M_w: weight average molecular weight (g/mol); M_n: number average molecular weight (g/mol).

Table 3
Kinetics of the GAX/DHP complexes hydrolysis by Tx-Xyl:SEC-$NaNO_3$ analysis of the evolution of the weight average molecular weight (M_w) of the GAX fraction as function of reaction times and determination of enzyme activity from reducing sugars quantification.

	M_w (of GAX) × 10^{-3} (g/mol)				
	GAX	GAX/DHP (4/0.25)	GAX/DHP (4/1)	GAX/DHP (4/4)	GAX/DHP (4/8)
Time (min)					
0	55.348	55.348	54.811	51.038	50.022
2	19.843	38.795	44.715	45.181	46.099
4	14.631	34.343	39.996	41.233	44.281
6	12.433	29.489	36.501	37.243	41.233
8	11.121	19.639	33.312	34.701	38.395
10	10.356	17.566	29.489	31.979	36.501
Endoxylanase[a]activity (IU/mL)	88.52 ± 5.66	64.07 ± 4.78	53.53 ± 5.12	36.76 ± 3.14	36.57 ± 2.26
Loss of activity (%)	0.00	27.62	39.52	58.47	58.69

[a] Results are mean values of duplicates (± standard error).

et al., 2007; Barakat, Winter, et al., 2007). As previously pointed out, this higher molar mass could be explained by a reinforced solubility of DHP, but also by the reactivity of coniferyl alcohol during the polymerization reaction.

To verify this hypothesis, the DHP extracted fractions were further characterized by thioacidolysis, which specifically cleaves the alkyl aryl ether bonds (β-*O*-4) that are formed during the polymerization of coniferyl alcohol (CA). The monomer yields thus closely reflect the frequency of lignin monomer units involved in β-*O*-4 only. The results reported in Table 2 indicate that the frequency of β-*O*-4 linked monomers was substantially lower in the case of DHP extracted from GAX-DHP (4/0.25) (154 μmol/g DHP) and progressively increased in line with the rise in DHP concentrations (*i.e.* 620 μmol/g DHP extracted from GAX-DHP (4/8)).

These results thus illustrated a different reactivity of CA during DHP polymerization as the monomer concentration increased. It is worth mentioning here that during the ZL polymerization process, the reaction starts with a coupling of monomeric radicals, leading to dimeric products (quinone methide). Some of these dimers associate rapidly (in bulk conditions) with larger molecules (tetramers, *etc.*), mainly *via* oxidation and β-β, β-5 coupling, but also to a lesser extent *via* β-*O*-4 coupling because of the exclusion of water molecules (Sarkanen, 1971). However, β-*O*-4 ether linkages are strongly favored in cross-coupling reactions (coupling of a monomer radical with the growing lignin oligomer/polymer) rather than in dehydrodimerization reactions. Such a feature is generally characteristic of endwise (Zutropf mode) polymerization (Ralph et al., 2004; Syrjanen & Brunow, 2000). Thus, the increase in the frequency of β-*O*-4 linkages in the DHP when using the ZL polymerization method suggests that oxidative polymerization mechanisms might evolve toward “endwise-like” mechanisms which more closely resemble lignification (Brunow et al., 1998) when the monomer (CA) concentration rises. One plausible explanation for this trend might be that the increase in the CA concentration in GAX solutions increases the hydrophobicity and density of the system. Interactions between GAX and the growing DHP, during the polymerization process, result in the formation of hydrophobic micro-domains (Barakat, Winter, et al., 2007). Therefore, the preferential location of nascent lignin oligomers in these hydrophobic micro-domains would allow continuous water removal during polymerization (Lairez et al., 2005). Hence, increasing the hydrophobicity of the system may promote frequent reactions between the oligomer phenoxy radical and the monomer β-radical, resulting in a DHP polymer with an enriched β-*O*-4 content.

Based on the SEC and thioacidolysis results, we suggest that the increase in the size of GAX-DHP particles may have been directly related to the increase in the molar mass of their elementary DHP constituents, as a result of improved solubility and the likely modified reactivity of DHP monomers. Overall, our results were somewhat analogous to those previously reported for covalent GAX-DHP nanocomposites with similar underlying mechanisms (Barakat, Chabbert, et al., 2007).

3.2. Enzymatic hydrolysis of GAX-DHP complexes

The GAX sample and the different GAX-DHP (4/0.25; 4/1; 4/4 and 4/8) model systems were subjected to the GH11 endoxylanase (Tx-Xyl). Hydrolysis kinetics were performed with small amounts of Tx-Xyl (0.04 IU/mg of GAX) to monitor the enzyme action pattern. The endoxylanase efficiency of each system was evaluated in terms of relative enzyme activity (IU/mL). The degree of enzymatic hydrolysis of the GAX fraction by the endoxylanase in each sample was also monitored as a function of incubation time, using SEC analysis operating under aqueous conditions.

3.2.1. Relative activity of Tx-Xyl on GAX-DHP complexes

The relative activity of endoxylanase (Tx-Xyl) on GAX and GAX-DHP model systems was determined by measuring the quantities of reducing sugars (xylose and xylo-oligosaccharides) released during 10 min of hydrolysis reaction and expressed as (IU/mL). The results are reported in Table 3. The maximum efficiency of Tx-Xyl (88.52 IU/mL) was achieved on the delignified GAX sample. Tx-Xyl was relatively efficient on the GAX sample, as a moderately branched polymer (arabinose/xylose *ratio* of 0.23). In contrast, the results indicated a gradual decrease in enzyme activity as the DHP content increased in the GAX-DHP systems. Indeed, the enzyme lost almost 28% and 39% of its initial activity on GAX in the case of GAX-DHP (4/0.25) and GAX-DHP (4/1), respectively, and nearly 58% with both GAX-DHP (4/4 and 4/8). Such results might have been expected because it is well recognized that lignins have a negative impact on the enzymatic hydrolysis of lignocellulosic substrates (Mooney, Mansfield, Touhy, & Saddler, 1998; Vinzant, Ehrman, Adney, Thomas, & Himmel, 1997; Zhu, O’Dwyer, Chang, Granda, & Holtzapple, 2008). There is abundant data in the literature regarding the impact of lignin on cellulases. By contrast, although fewer studies have dealt directly with this subject in the case of xylanases, similar conclusions have been drawn. Senior et al. investigated the recovery of enzyme activity after the interaction of a xylanase from *T. harzianum E58* with various substrates containing lignin (unbleached sulfite pulp, *etc.*). They found that substrates with higher lignin content caused the greatest loss in activity. These authors suggested that the loss of enzyme activity could be caused by either the binding of enzymes onto insoluble lignin or the inactivation by soluble materials leaching out of the pulps (Senior, Mayers, Breuil, & Saddler, 1990).

The results presented herein concerning GAX-DHP model systems are consistent with the results obtained by Senior et al. We can therefore hypothesize that the loss of Tx-Xyl activity may have been due to non-productive interactions between the enzyme

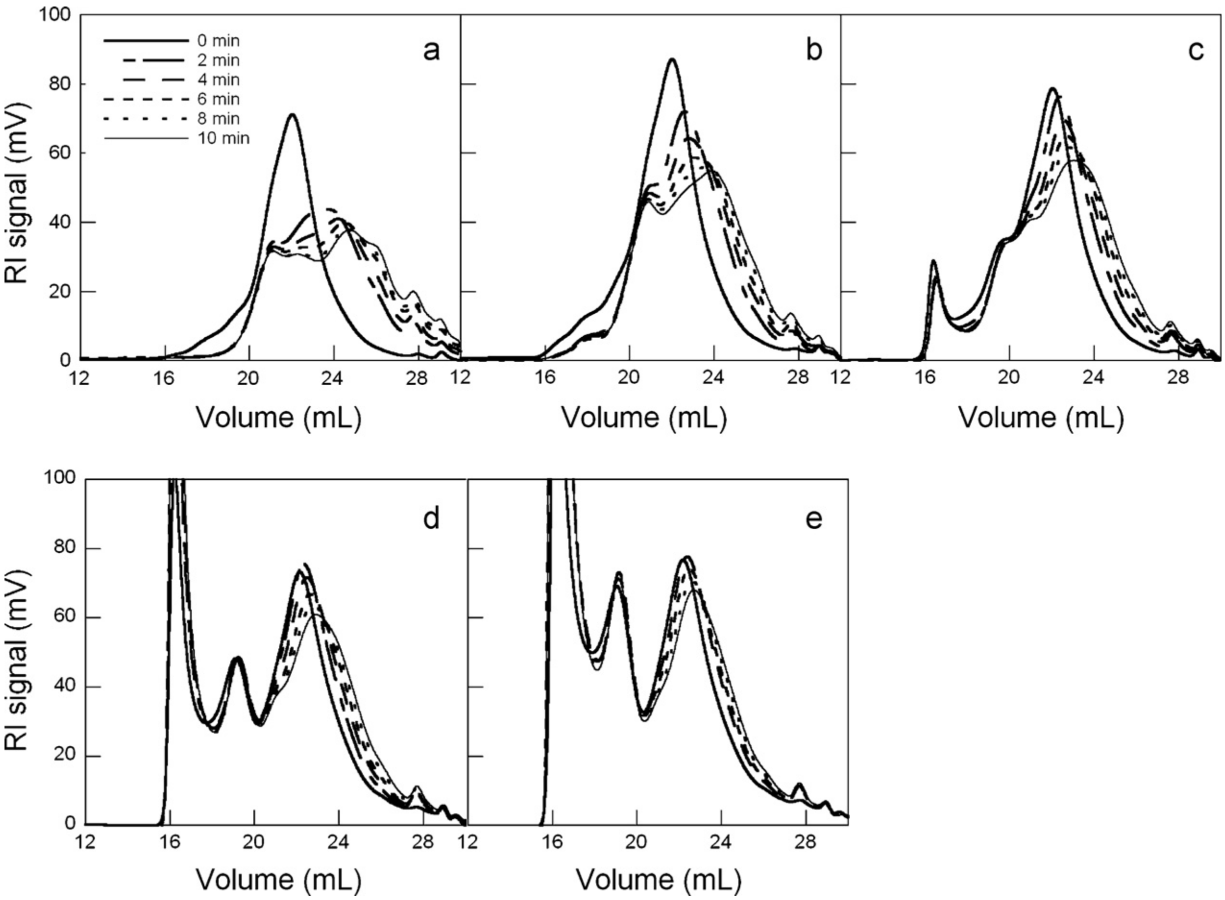

Fig. 4. Hydrolysis kinetics of (a) GAX, (b) GAX-DHP (4/0.25), (c) GAX-DHP (4/1), (d) GAX-DHP (4/4) and (e) GAX-DHP (4/8) by Tx-Xyl (0.04 IU/mg GAX). SEC-$NaNO_3$ elution profiles at different reaction times.

and the rising DHP content. Moreover, the increase in the size of DHP and corresponding GAX-DHP complexes may have induced an increase in the surface area available for the non-productive binding of xylanase and/or an increase in the amounts of reactive functions (*i.e.* hydroxyl functional groups) that could interfere with enzyme functionality (*i.e.* through an inhibition/inactivation mechanism) (Boukari, O'Donohue, Rémond, & Chabbert, 2011; Kawamoto, Nakatsubo, & Murakami, 1992; Pan, 2008).

3.2.2. SEC monitoring of the hydrolysis kinetics of GAX-DHP complexes by Tx-Xyl

To study Tx-Xyl activity patterns as a function of the DHP content, the degree of enzymatic hydrolysis of the GAX fraction in each GAX-DHP model system was monitored as a function of incubation time, using SEC analysis operating under aqueous conditions with RI detection (Fig. 4). The elution profiles showed a progressive shift of the GAX peak toward lower molar masses during the course of endoxylanase-mediated hydrolysis, which was indicative of GAX depolymerization and the formation of low molecular weight products. However, when comparing the action of the enzyme on the different GAX-DHP model systems, the degree of the GAX hydrolysis became less marked as the DHP content rose, as could be deduced from the decline of RI signal intensity and elution volume. Likewise, and especially in the case of the GAX-DHP (4/8) nanocomposite (Fig. 4e), the GAX fraction was only weakly affected by action of the enzyme. The evolution of the average molecular weight in the GAX fraction was monitored during the kinetics, using a calculation based on pullulan standard calibration. The M_w values are reported in Table 3. From the results, it can be seen that the delignified GAX sample was the most effectively degraded by Tx-Xyl, since after 10 min the level of polymer M_w fell from 55.348 to 10.356 g/mol, while comparatively, as the DHP content rose, enzyme action gradually decreased, as can be deduced from the increase in M_w in the residual GAX fraction (17.566; 29.489; 31.979 and 36.501 g/mol for GAX-DHP 4/0.25; 4/1; 4/4 and 4/8, respectively). These results thus revealed increasingly limited accessibility within the enzyme–substrate system during the reaction, most likely due to either a lack of accessibility of the GAX substrate to the enzyme, or inversely of the enzyme to the substrate. Considering that all enzymatic reactions were performed with a high substrate to enzyme *ratio* and that the supramolecular organization of the different non covalent GAX-DHP model systems would not presumably pose any physical hindrance to GAX access (Boukari et al., 2009), we can assume that the second suggestion is the most plausible. Hence, the increasingly limited accessibility of Tx-Xyl to the GAX substrate as the DHP content rose may have resulted from non-productive interactions between the enzyme and the increasingly available interacting surfaces of GAX-DHP globules. According to the suggestions made by Senior et al., such interactions would limit xylanase action by reducing the effective concentrations of the enzyme, and also prevent its resolubilization, thereby restricting its recyclability during the hydrolysis reaction (Senior, Mayers, Breuil, & Saddler, 1990).

The non-specific adsorption or binding of cellulases and hemicellulases to the surface of lignin has often been proposed as the main mechanism leading to a loss of enzyme activity and thus to a decline in the hydrolysis rates of lignocellulosic substrates (Converse, Ooshima, & Burns, 1990; Palonen, Tjerneld, Zacchi, & Tenkanen, 2004; Sutcliffe & Saddler, 1986). The hydrophobicity of the lignin surface has generally been regarded as a very important factor; the more hydrophobic the surface, the higher the degree of adsorption, although electrostatic interactions may interfere with this trend. Recently, Berlin et al. examined the inhibition of a broad panel of hydrolytic enzymes (cellulases, β-glucosidases and xylanases from *Trichoderma*, *Penicillium* and *Aspergillus spp.* culture filtrates) by two lignins. The authors correlated the differences in the adsorption behavior of the enzymes with differences in the chemical interactions between enzymes and lignin, but little is known of the exact nature of these interactions (Berlin et al., 2006).

Our results tended to highlight the impact of the surface areas and particle sizes of GAX-DHP globules on endoxylanase activity, suggesting that a surface interaction phenomenon (such as non-specific adsorption) was most likely. The chemical structure of lignin (the proportion of intermonomer linkages and the type of monomer) may alter these surface areas. Nevertheless, the action of the enzyme could also be hampered by a potential catalytic inhibition through interactions with soluble aromatic compounds (Boukari, O'Donohue, Rémond, & Chabbert, 2011). Further investigation of the role of the surface interfacial behavior of the protein in the biocatalysis of such heterologous systems is necessary to understand the process of enzyme adsorption on lignins.

4. Conclusion

Variations in the lignin content and particle size parameters of lignocelluloses were successfully modeled using *in vitro* reconstituted GAX-DHP model systems. Characterization of these systems revealed that growing DHP in GAX solutions form GAX-DHP complexes which presumably behave like globular particles. Particle size may be directly related to the initial monolignol concentration that could affect the oxidative polymerization mechanisms of monolignols, as evidenced by variations in the proportion of *β-O*-4 linkages. The susceptibility of GAX-DHP model systems to the action of GH11 endoxylanase (Tx-Xyl) was then evaluated. The results highlighted the negative impact of the lignin (DHP) content on enzyme activity and suggested that the particle size and surface area of GAX-DHP complexes may be important factors affecting enzyme availability and effectiveness. Future work will focus on studying macromolecular changes affecting the endoxylanase during interactions with phenolic components, as well as protein partition parameters and interfacial behavior within heterologous carbohydrate–lignin systems (Tu et al., 2007) in order to understand in greater detail the precise nature of non-specific lignin–endoxylanase interactions.

Acknowledgments

The authors gratefully acknowledge the Champagne-Ardenne Regional Council (France) for its financial support for the PhD project by I. Boukari, D. Crônier for mass spectrometry analysis, and J. Michel and L. Wortham (Laboratoire de Microscopie Electronique Analytique, Université de Reims Champagne-Ardenne, France) for their helpful contribution to TEM analyses.

References

Anderson, W., & Akin, D. (2008). Structural and chemical properties of grass lignocelluloses related to conversion for biofuels. *Journal of Industrial Microbiology and Biotechnology*, *35*, 355–366.

Barakat, A., Chabbert, B., & Cathala, B. (2007). Effect of reaction media concentration on the solubility and the chemical structure of lignin model compounds. *Phytochemistry*, *68*, 2118–2125.

Barakat, A., Winter, H., Rondeau-Mouro, C., Saake, B., Chabbert, B., & Cathala, B. (2007). Studies of xylan interactions and cross-linking to synthetic lignins formed by bulk and end-wise polymerization: A model study of lignin carbohydrate complex formation. *Planta*, *226*, 267–281.

Berlin, A., Balakshin, M., Gilkes, N., Kadla, J., Maximenko, V., Kubo, S., & Saddler, J. (2006). Inhibition of cellulase, xylanase and β-glucosidase activities by softwood lignin preparations. *Journal of Biotechnology*, *125*, 198–209.

Boukari, I., Putaux, J.-L., Cathala, B., Barakat, A., Saake, B., Rémond, C., O'Donohue, M., & Chabbert, B. (2009). In vitro model assemblies to study the impact of lignin–carbohydrate interactions on the enzymatic conversion of xylan. *Biomacromolecules*, *10*, 2489–2498.

Boukari, I., O'Donohue, M., Remond, C., & Chabbert, B. (2011). Probing a family GH11 endo-beta-1,4-xylanase inhibition mechanism by phenolic compounds: Role of functional phenolic groups. *Journal of Molecular Catalysis B: Enzymatic*, *72*, 130–138.

Brunow, G. S., Kilpeläinen, I., Sipilä, J., Syrjänen, K., Karhunen, P., Setälä, H., & Rummakko, P. (1998). Oxidative coupling of phenols and the biosynthesis of lignin. In *Lignin and lignan biosynthesis*. American Chemical Society., pp. 131–147.

Cathala, B., & Monties, B. (2001). Influence of pectins on the solubility and the molar mass distribution of dehydrogenative polymers (DHPs, lignin model compounds). *International Journal of Biological Macromolecules*, *29*, 45–51.

Cathala, B., Saake, B., Faix, O., & Monties, B. (1998). Evaluation of the reproducibility of the synthesis of dehydrogenation polymer models of lignin. *Polymer Degradation and Stability*, *59*, 65–69.

Chandra, R. P., Bura, R., Mabee, W. E., Berlin, A., Pan, X., & Saddler, J. N. (2007). Substrate pretreatment: The key to effective enzymatic hydrolysis of lignocellulosics. *Advances in Biochemical Engineering/Biotechnology*, *108*, 67–93.

Chang, V., & Holtzapple, M. (2000). Fundamental factors affecting biomass enzymatic reactivity. *Applied Biochemistry and Biotechnology*, *84/86*, 5–37.

Chum, H. L., Johnson, D. K., Tucker, M. P., & Himmel, M. E. (1987). Some aspects of lignin characterization by high performance size exclusion chromatography using styrene divinylbenzene copolymer gels. *Holzforschung*, *41*, 97–108.

Converse, A., Ooshima, H., & Burns, D. (1990). Kinetics of enzymatic hydrolysis of lignocellulosic materials based on surface area of cellulose accessible to enzyme and enzyme adsorption on lignin and cellulose. *Applied Biochemistry and Biotechnology*, *24–25*, 67–73.

Courtin, C. M., Van den Broeck, H., & Delcour, J. A. (2000). Determination of reducing end sugar residues in oligo- and polysaccharides by gas–liquid chromatography. *Journal of Chromatography A*, *866*, 97–104.

Debeire-Gosselin, M., Loonis, M., Samain, E., & Debeire, P. (1992). Purification and properties of a 22 kDa endoxylanase excreted by a new strain of thermophilic Bacillus. In J. Visser, G. Beldman, M. A. Kusters-van Someren, & A. G. J. Voragen (Eds.), *Xylans and xylanases* (pp. 463–466). Amsterdam: Elsevier Science Publishers.

Draude, K. M., Kurniawan, C. B., & Duff, S. T. B. (2001). Effect of oxygen delignification on the rate and extent of enzymatic hydrolysis of lignocellulosic material. *Bioresource Technology*, *79*, 113–120.

Faix, O., & Lange, W. (1981). Molecular weight determinations of DHP's from mixtures of precursors by steric exclusion chromatography (HPLC). *Holzforschung*, *35*, 137–140.

Freudenberg, K., & Neish, A. (1968). Biosynthesis of lignin. *Berlin*.

Higuchi, T., Ogino, K., & Tanahashi, M. (1971). Effect of polysaccharides on dehydropolymerization of coniferyl alcohol. *Wood Research*, *51*, 1–11.

Kawamoto, H., Nakatsubo, F., & Murakami, K. (1992). Protein-adsorbing capacities of lignin samples. *Mokuzai Gakkaishi*, *38*, 81–84.

Kaya, F., Heitmann, J., & Joyce, T. (1999). Effect of dissolved lignin and related compounds on the enzymatic hydrolysis of cellulose model compound. *Cellulose Chemistry and Technology*, *33*, 203–213.

Lairez, D., Cathala, B., Monties, B., Bedos-Belval, F., Duran, D., & Gorrichon, L. (2005). On the first steps of lignification: Aggregation during coniferyl alcohol polymerisation in pectin solution. *Biomacromolecules*, *6*, 763–774.

Lapierre, C. (1993). Application of new methods for the investigation of lignin structure. In H. G. Jung, D. R. Buxton, R. D. Hatfield, & J. Ralph (Eds.), *Forage cell wall structure and digestibility* (pp. 133–166). Madison: ASA, CSSA, and SSSA.

Lapierre, C., Monties, B., & Rolando, C. (1986). Thioacidolysis of poplar lignins: Identification of monomeric syringyl products and characterisation of guaiacyl-syringyl lignins fractions. *Holzforschung*, *40*, 113–118.

Ludley, F. H., & Ralph, J. (1996). Improved preparation of coniferyl and sinapyls alcohols. *Journal of Agricultural and Food Chemistry*, *44*, 2942–2943.

McKendry, P. (2002). Energy production from biomass (part 1): Overview of biomass. *Bioresource Technology*, *83*, 37–46.

Micic, M., Radotic, K., Jeremic, M., Djikanovic, D., & Kämmer, S. B. (2004). Study of the lignin model compound supramolecular structure by combination of near-field scanning optical microscopy and atomic force microscope. *Colloids and Surfaces B: Biointerfaces*, *34*, 33–40.

Micic, M., Radotic, K., Jeremic, M., & Leblanc, R. M. (2003). Study of self-assembly of the lignin model compound on cellulose model substrate. *Macromolecular Bioscience*, *3*, 100–106.

Mooney, C. A., Mansfield, S. D., Touhy, M. G., & Saddler, J. N. (1998). The effect of the initial pore volume and lignin content on the enzymatic hydrolysis of softwoods. *Bioresource Technology*, *64*, 113–119.

Palonen, H., Tjerneld, F., Zacchi, G., & Tenkanen, M. (2004). Adsorption of *Trichoderma reesei* CBH I and EG II and their catalytic domains on steam pretreated softwood and isolated lignin. *Journal of Biotechnology*, *107*, 65–72.

Pan, X. (2008). Role of functional groups in lignin inhibition of enzymatic hydrolysis of cellulose to glucose. *Journal of Biobased Materials and Bioenergy*, *2*, 25–32.

Putaux, J.-L., Buléon, A., Borsali, R., & Chanzy, H. (1999). Ultrastructural aspects of phytoglycogen from cryo-transmission electron microscopy and quasi-elastic light scattering data. *International Journal of Biological Macromolecules*, *26*, 145–150.

Radotic, K., Micic, M., & Jeremic, M. (2005). New insights into the structural organization of the plant polymer lignin. *Annals of the New York Academy of Sciences*, *1048*, 215–229.

Ralph, J., Lundquist, K., Brunow, G., Lu, F., Kim, H., Schatz, P. F., Marita, J. M., Hatfield, R. D., Ralph, S. A., Christensen, J. H., & Boerjan, W. (2004). Lignins: Natural polymers from oxidative coupling of 4-hydroxyphenyl-propanoids. *Phytochemistry Reviews*, *3*, 29–60.

Saake, B., Argyropoulos, D. S., Beinhoff, O., & Faix, O. (1996). A Comparison of lignin polymer models (DHPs) and lignins by ^{31}P NMR spectroscopy. *Phytochemistry*, *43*, 499–507.

Samain, E., Debeire, P., & Touzel, J. P. (1997). High level production of a cellulase-free xylanase in glucose-limited fed batch cultures of a thermophilic Bacillus strain. *Journal of Biotechnology*, *58*, 71–78.

Samain, E., Touzel, J. P., Brodel, B., & Debeire, P. (1992). Isolation of a thermophilic bacterium producing high level of xylanase. In *Xylans and xylanases*. Amsterdam: Elsevier Science Publishers B.V., pp. 467–470.

Sarkanen, K. V. (1971). Precursors and their polymerization. In K. V. Sarkanen, & C. H. Ludwig (Eds.), *Lignins, occurrence, formation, structure and reactions* (pp. 95–163). New York: Wiley-Interscience.

Senior, D. J., Mayers, P. R., Breuil, C., & Saddler, J. N. (1990). The interaction of xylanase with pulps: Non-selective adsorption and inactivation of xylanase. In T. K. Kirk, & H.-M. Chang (Eds.), *Biotechnology in pulp and paper manufacture* (pp. 169–182). Boston: Butterworth-Heinemann.

Shigematsu, M., Goto, A., Yoshida, S., Tanashi, M., & Shinoda, Y. (1994). Affinities of monolignols and saccharides determined by the solubility method. *Mokuzai Gakkaishi*, *40*, 321–327.

Sutcliffe, R., & Saddler, J. N. (1986). The role of lignin in the adsorption of cellulases during enzymatic treatment of lignocellulosic material. *Biotechnology & Bioengineering Symposium*, *17*, 749–762.

Syrjanen, K., & Brunow, G. (2000). Regioselectivity in lignin biosynthesis. The influence of dimerization and cross-coupling. *Journal of the Chemical Society-Perkin Transactions*, *1*, 183–187.

Tanahashi, T., & Higuchi, A. T. (1982). Dehydrogenative polymerization of monolignols by peroxidase and H_2O_2 in a dialysis tube. *Holzforschung*, *36*, 117–122.

Tu, M., Chandra, R. P., & Saddler, J. N. (2007). Evaluating the distribution of cellulases and the recycling of free cellulases during the hydrolysis of lignocellulosic substrates. *Biotechnology Progress*, *23*, 398–406.

Vinzant, T., Ehrman, C., Adney, W., Thomas, S., & Himmel, M. (1997). Simultaneous saccharification and fermentation of pretreated hardwoods: Effect of native lignin content. *Applied Biochemistry and Biotechnology*, *62*, 99–104.

Winter, H., Barakat, A., Cathala, B., & Saake, B. (2006). Preparation of arabinoxylan and its sorption on bacterial cellulose during cultivation. *Macromolecular Symposia*, *232*, 74–84.

Wyman, C. E. (2003). Potential synergies and challenges in refining cellulosic biomass to fuels, chemicals and power. *Biotechnology Progress*, *19*, 254–262.

Zhu, L., O'Dwyer, J. P., Chang, V. S., Granda, C. B., & Holtzapple, M. T. (2008). Structural features affecting biomass enzymatic digestibility. *Bioresource Technology*, *99*, 3817–3828.